*Journal of Ceramic Processing Research. Vol. 19, No. 1, pp. 65~68 (2018)*

J O U R N A L O F
**Ceramic Processing Research**

# Inductively coupled plasma etching of high-k dielectric $HfSiO_4$ film

**Byoung Su Choi[a], Hae Chan Kim[a], Jin Kon Kim[b], Jeong Seog Kim[c], Jeong Ho Ryu[d], and Hyun Cho[b,*]**
[a]*Department of Nano Fusion Technology, Pusan National University, Gyeongnam 50463, Korea*
[b]*Department of Nanomechatronics Engineering, Pusan National University, Busan 46241, Korea*
[c]*NEXTOP KOREA Co. Ltd., Gyeongnam 51120, Korea*
[d]*Department of Materials Science and Engineering, Korea National University of Transportation, Chungbuk 27469, Korea*

**Hafnium silicate ($HfSiO_4$) is one of the leading high-k dielectrics for advanced complementary metal oxide semiconductor field-effect transistors (CMOSFETs) since it can provide the reduced leakage current characteristics while maintaining the same gate capacitance in sub-2 nm equivalent oxide thickness regime. High resolution pattern transfer of the $HfSiO_4$-based gate structure is important to achieve a good device performance. High density plasma etching of the $HfSiO_4$ thin film was performed in $Cl_2$/Ar and $SF_6$/Ar inductively coupled plasmas (ICPs) and the effect of plasma composition, ICP source power and rf chuck power on the $HfSiO_4$ etch characteristics was studied. As the concentration of fluorine in the $SF_6$/Ar ICP discharges increases, a steady increase of the $HfSiO_4$ etch rate was observed while the $HfSiO_4$ etch rate in the $Cl_2$/Ar discharges decreased at the chlorine content beyond ~33%. For both plasma chemistries, the $HfSiO_4$ etch rate generally increased as the ICP source power or rf chuck power increased under most of the conditions examined and maximum etch rates of ~921 Å/min and ~776 Å/min were obtained in the $5SF_6/10Ar$ and $5Cl_2/10Ar$ ICP discharges, respectively. The $5Cl_2/10Ar$ ICP discharges produced better surface morphology with the normalized roughness values in the rage of 0.72-1.32 compared to the $5SF_6/10Ar$ plasmas. Highly anisotropic pattern transfer was performed with the $5SF_6/10Ar$ ICP discharges.**

**Key words: $HfSiO_4$ thin film, Inductively coupled plasma etching, $Cl_2$/Ar and $SF_6$/Ar inductively coupled plasmas, Etch rate, anisotropy.**

## Introduction

The reduction of dimensions in Si-based complementary metal oxide semiconductor (CMOS) transistors continued for the past few decades has pushed silicon dioxide ($SiO_2$) gate dielectric close to its physical limit. As device dimension approaches to sub-45 nm scale, the equivalent oxide thickness (EOT) of the conventional $SiO_2$ dielectrics are required to be smaller than 1 nm. However, the $SiO_2$ dielectric layers thinner than ~2 nm would have a significant power dissipation attributed to leakage current over 1 $A \cdot cm^{-2}$ due to direct tunneling through the oxide, which is not acceptable for the CMOS devices. In order to extend the downward scaling of the gate dielectric to the sub-1 nm regime, oxides with high dielectric constant has been suggested as a solution that maintains the same gate capacitance without increasing the leakage current [1-5]. The high-k gate dielectric should meet the requirements such as high stability with semiconductor layer, high recrystallization temperature, low interface trap densities, smooth and conformal deposition morphology, high resistance to diffusion of dopants, and sufficient band offsets for charge carriers [6-10]. Among various materials, hafnium silicate ($HfSiO_4$) is one of the leading high-k dielectrics that can readily satisfy those requirements for advanced CMOS devices [11-17]. In addition, $HfSiO_4$ has recently been considered as one of the potential candidates for gate dielectric for $InGaZnO_4$- and $Ga_2O_3$-based MOSFETs [18, 19].

In the fabrication of the $HfSiO_4$-based gate structure with very fine dimensions, a precise pattern transfer is essential to achieve a reduced contact resistance and a good device performance. Pattern transfer of $HfSiO_4$ dielectric layer is required to be an anisotropic feature formation with high resolution, residue-free and low ion-induced damage. High density plasma etching is the most commonly used pattern transfer technique in the semiconductor industry, which can meet these requirements. Up to the present, little work has been reported on the plasma etching of $HfSiO_4$ film [20]. In this work, we report on the high density plasma etching of high-k dielectric $HfSiO_4$ films in chlorine- and fluorine-based ($Cl_2$/Ar and $SF_6$/Ar) inductively coupled plasmas (ICPs). The effect of plasma composition, ion flux and ion energy on the $HfSiO_4$ etch characteristics was studied.

## Experimental

~1 μm thick $HfSiO_4$ films were deposited on the Φ4" Si substrates by rf magnetron sputtering with a

*Corresponding author:
Tel : +82-51-510-6113
Fax: +82-51-514-2358
E-mail: hyuncho@pusan.ac.kr

commercial Φ3" sputter target. As-deposited $HfSiO_4$ films were patterned with either AZ 5214 photoresist or ~500 Å thick nickel layer. High density plasma etching was performed in a planar inductively coupled plasma source operating at 13.56 MHz and power up to 1000 W, and the samples were thermally bonded to a Si carrier wafer that was mechanically clamped to a He backside-cooled, rf-powered (13.56 MHz, up to 450W) chuck. $Cl_2$/Ar and $SF_6$/Ar inductively coupled plasmas were employed to etch the patterned $HfSiO_4$ films and process pressure was maintained at 10 mTorr, with a gas load of 15 standard cubic centimeters per minute (sccm). After removal of the mask materials, etch rates were measured by stylus profilometry. The surface morphology was characterized by tapping mode atomic force microscopy (AFM) and the anisotropy of etched features was examined by field-emission scanning electron microscopy (FE-SEM).

## Results and Discussion

Fig. 1 shows the effect of plasma composition on the $HfSiO_4$ etch rate in $Cl_2$/Ar and $SF_6$/Ar ICP discharges at a fixed source power (700 W), rf chuck power (100 W) and pressure (10 mTorr). The dc self-bias in both $Cl_2$/Ar and $SF_6$/Ar ICP discharges increases as the percentage of $Cl_2$ and $SF_6$ increase due to the electronegative character of chlorine and fluorine, and this indicates that the ion density in the plasma decreases under the conditions examined. In $Cl_2$/Ar ICP discharges, the $HfSiO_4$ etch rate initially increases as the concentration of $Cl_2$ in the discharges increases up to 33% and then decreases slightly as the $Cl_2$ content increases further. This indicates that the etching of $HfSiO_4$ under these conditions is limited by physical component of the etching. As the $Cl_2$ content increases beyond 33%, a chlorinated selvedge layer is accumulated on the surface and ion-assisted removal of this layer retards further etching due to the reduced ion density in the plasma. On the contrary, the $HfSiO_4$ etch rate increases monotonically as the $SF_6$ content in the discharges increases, suggesting that the neutral-to-ion ratio in the $SF_6$/Ar ICP discharges is still sustained within the optimal range where the formation of the metal fluoride etch products ($HfF_x$ and $SiF_x$) is balanced with the subsequent ion-assisted desorption.

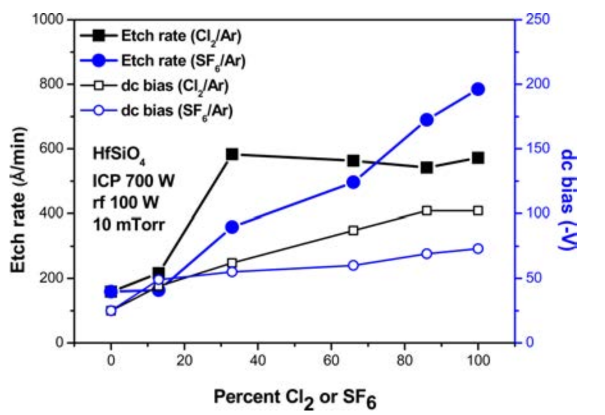


**Fig. 1.** $HfSiO_4$ etch rates as a function of plasma composition in $Cl_2$/Ar and $SF_6$/Ar ICP discharges (700 W ICP source power, 100 W rf chuck power, 10 mTorr pressure).

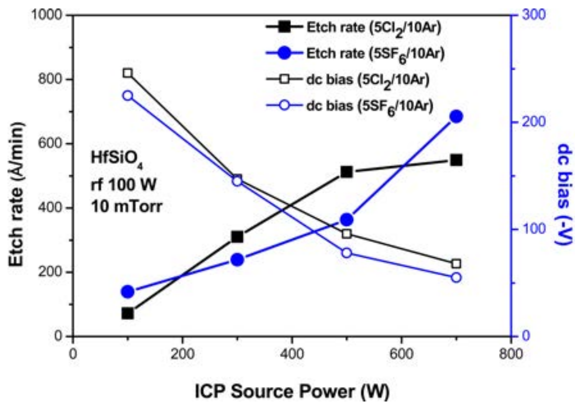


**Fig. 2.** $HfSiO_4$ etch rates as a function of ICP source power in $5Cl_2$/10Ar and $5SF_6$/10Ar ICP discharges (100 W rf chuck power, 10 mTorr pressure).

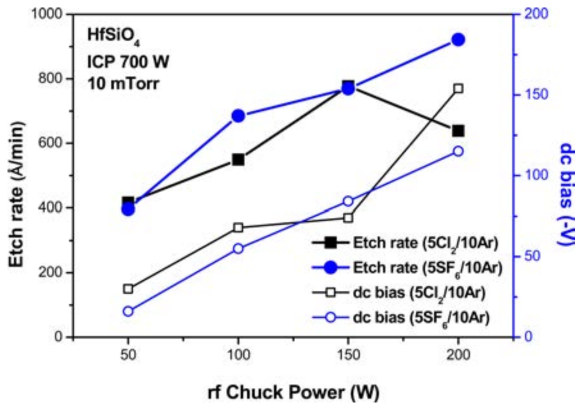


**Fig. 3.** $HfSiO_4$ etch rates as a function of rf chuck power in $5Cl_2$/10Ar and $5SF_6$/10Ar ICP discharges (700 W ICP source power, 10 mTorr pressure).

The effect of ICP source power on the $HfSiO_4$ etch rate in $Cl_2$/Ar and $SF_6$/Ar ICP discharges at fixed plasma composition, rf chuck power (100 W) and pressure (10 mTorr) is shown in Fig. 2. For both plasma chemistries, the $HfSiO_4$ etch rate increases continuously as the ICP source power increases due to the increased atomic chlorine or fluorine density and ion flux in the discharges. This is consistent with an etch mechanism in which the formation of metal chloride or metal fluoride etch products by the chemical reaction between the component elements of the $HfSiO_4$ film and the adsorbed chlorine or fluorine neutrals should be balanced with the ion-assisted desorption of the etch products. No significant difference in the $HfSiO_4$ etch rate was observed for these two plasma chemistries and this is presumably because there is no significant difference in the volatility between the potential metal chloride and metal fluoride etch products (presumably $HfCl_4$; m.p. 432 ºC, $HfF_4$; b.p. 970 ºC, $SiCl_4$; b.p.

57.65 °C, $SiF_4$; b.p. -86 °C) [21]. Maximum etch rates of ~700 Å/min and ~550 Å/min were obtained at 700 W source power in the $5SF_6/10Ar$ and $5Cl_2/10Ar$ ICP discharges, respectively.

Fig. 3 shows the rf chuck power dependence of the $HfSiO_4$ etch rate for chlorine- and fluorine-based ICP discharges at a fixed source power (700 W) and pressure (10 mTorr). For $5SF_6/10Ar$ ICP discharges, the $HfSiO_4$ etch rate increases continuously as rf chuck power increases, indicating the presence of the physical component of the etching. The average energy of the $Ar^+$ ions that impinging on the $HfSiO_4$ surface increases in proportion to the rf chuck power, and this enhances the ion-assisted removal of the metal fluoride etch products from the surface. The rate-limiting step under these conditions would be the $HfF_x$ and $SiF_x$ etch products formation by the chemical reaction between the $HfSiO_4$ surface atoms and the adsorbed fluorine neutrals. For $5Cl_2/10Ar$ ICP discharges, the $HfSiO_4$ etch rate initially increases as the rf chuck power increases up to 150 W, and then decreases at 200 W due to the ion-assisted desorption of the reactive chlorine neutrals before they complete a chemical reaction with the $HfSiO_4$ surface atoms. Maximum etch rates of ~921 Å/min and ~776 Å/min were produced in the $5SF_6/10Ar$ and $5Cl_2/10Ar$ ICP discharges, respectively.

Fig. 4 presents the AFM scan images of the $HfSiO_4$ surfaces etched in $5Cl_2/10Ar$ and $5SF_6/10Ar$ ICP discharges as a function of rf chuck power at a fixed source power (700 W) and pressure (10 mTorr). In each sample, the etch depth was maintained at ~2000 Å and root-mean-square (RMS) roughness of the unetched $HfSiO_4$ control sample was ~1.38 nm. For $5Cl_2/10Ar$ ICP discharges, the etched $HfSiO_4$ samples show similar or better surface roughness values compared to the unetched control sample under the conditions examined, and the surface morphology is improved as the rf chuck power increases because of the ion-enhanced removal of sharp features from the surface. However, degradation in the surface morphology with the normalized roughness ranging from 1.04 to 1.73 compared to the unetched surface was observed for $5SF_6/10Ar$ discharges. This is most likely due to the relatively inhomogeneous removal of surface atoms by the ion bombardments. This result suggests that $5Cl_2/10Ar$ ICP etching of the $HfSiO_4$ layer would be a reasonable choice if a smooth surface morphology is needed.

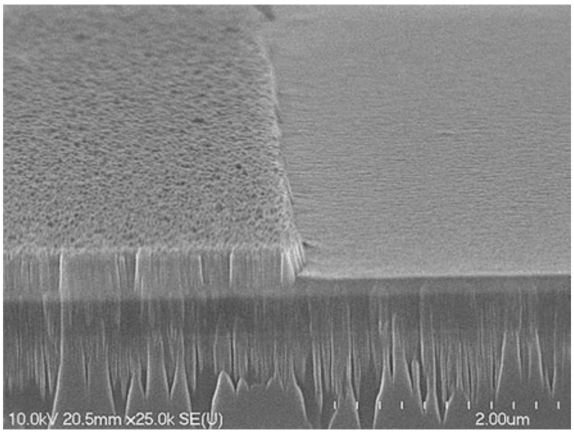


**Fig. 5.** A SEM micrograph of the feature etched into $HfSiO_4$ using $5SF_6/10Ar$ ICP discharges (500 W ICP source power, 100 W rf chuck power, 10 mTorr pressure).

Fig. 5 shows a FE-SEM micrograph of feature etched into $HfSiO_4$ films using the $5SF_6/10Ar$ ICP discharges with a 500 W source power, 100 W rf chuck power, and 10 mTorr pressure. Please note that the Ni mask layer is still in place and the etch depth was maintained at ~2500 Å. It can be seen that a pattern transfer with high anisotropy was performed with the $5SF_6/10Ar$ ICP discharges and the etched $HfSiO_4$ surface shows a smooth surface morphology.

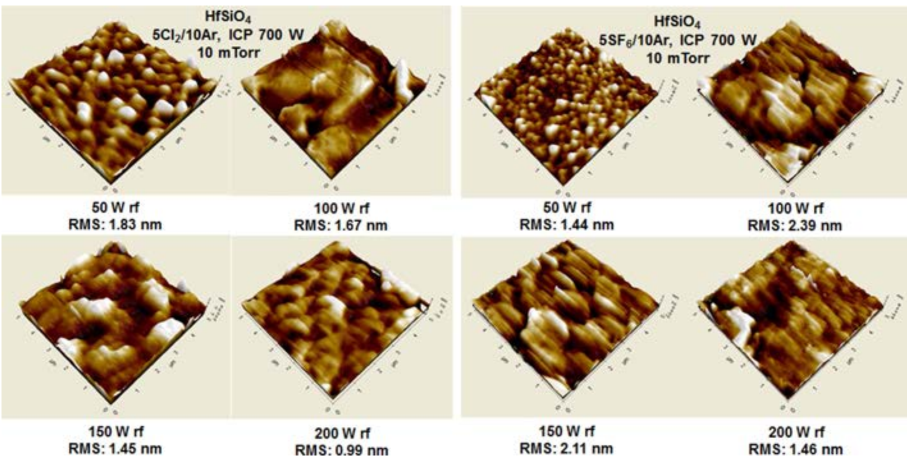


**Fig. 4.** AFM surface scan imges of $HfSiO_4$ films etched in $5Cl_2/10Ar$ and $5SF_6/10Ar$ ICP discharges (700 W ICP source power, 10 mTorr pressure).

## Conclusions

High density plasma etching of the high-k dielectric $HfSiO_4$ thin film was performed in the $Cl_2$/Ar and $SF_6$/Ar inductively coupled plasmas, and the effect of process variables on the etch characteristics were examined. The $HfSiO_4$ etch rate increased steadily as the $SF_6$ concentration in the $SF_6$/Ar ICP discharges increased due to maintaining the balance between the metal fluoride etch product formation and subsequent ion-assisted desorption, while the $HfSiO_4$ etch rate in the $Cl_2$/Ar discharges decreased at the chlorine concentrations beyond ~33%. Practical and controllable $HfSiO_4$ etch rates were obtained in both $5SF_6$/10Ar and $5Cl_2$/10Ar ICP discharges and a significant difference in the $HfSiO_4$ etch rate between these two plasma chemistries was not observed. For the $5SF_6$/10Ar ICP discharges, the $HfSiO_4$ etch rate showed a strong dependence on the ICP source power and rf chuck power, and a maximum etch rate of ~921 Å/min was obtained. A similar trend was observed for the $5Cl_2$/10Ar ICP discharges under most the conditions examined, but the $HfSiO_4$ etch rate decreased at the highest rf chuck power (200 W) due to the enhanced ion-assisted removal of reactive chlorine neutrals before they can react with the surface atoms. The $HfSiO_4$ films etched in the $5Cl_2$/10Ar ICP discharges showed similar or better surface roughness values compared to the unetched surface while a slight degradation in the surface morphology was observed for the samples etched in the $5SF_6$/10Ar ICP discharges. Pattern transfer using the $5SF_6$/10Ar ICP discharges with a moderate source power (500 W) and low rf chuck power (100 W) produced an highly anisotropic etched feature into the $HfSiO_4$ film.

## References


1. B.R. Kumar and T.S. Rao, Int. J. Pure Appl. Sci. Technol. 4 (2011) 105-114.
2. R. Chau, S. Datta, M. Doczy, B. Doyle, J. Kavalieros, and M. Metz, IEEE Electron Dev. Lett. 25 (2004) 408-410.
3. S.H. Jeong, I.S. Bae, Y.S. Shin, S.-B. Lee, H.-T. Kwak, and J.-H. Boo, Thin Solid Films 475 (2005) 354-358.
4. J. Robertson, Rep. Prog. Phys. 69 (2006) 327-396.
5. Z.J. Luo, X. Guo, T.P. Ma, and T. Tamagawa, Appl. Phys. Lett. 79 (2001) 2803-2804.
6. G.D. Wilk, R.M. Wallace, and J.M. Anthony, J. Appl. Phys. 89 (2001) 5243-5275.
7. H.S. Kim, S.A. Campbell, and D.C. Gilmer, IEEE Electron. Dev. Lett. 18 (1997) 465-467.
8. S.J. Wang, C.K. Ong, S.Y. Xu, P. Chen, W.C. Tjiu, ACH. Huan, W.J. Yoo, J.S. Lim, W. Feng, and W.K. Choi, Semicond. Sci. Technol. 16 (2001) L13-L16.
9. D. Han, J. Kang, C. Lin, and R. Han, Chin. Phys. 12 (2003) 325-327.
10. G.D. Wilk and R.M. Wallace, Appl. Phys. Lett. 76 (2000) 112-114.
11. I.Z. Mitrovic, O. Buiu, S. Hall, C. Bungey, T. Wagner, W. Davey and Y. Lu, Microel. Rel. 47 (2007) 645-648.
12. K. Xiong, Y. Du, K. Tse, and J. Robertson, J. Appl. Phys. 101 (2007) 024101 (024101-1~024101-7).
13. H.K. Dong and L.B. Shi, Chin. Phys. Lett. 33 (2016) 016101 (016101-1~016101-4).
14. L. Zhao, M. Nelson, H. Aldridge, T. Lamsasri, C.M. Fancher, J.S. Forrester, T. Nishida, S. Moghaddam, and J.L. Jones, J. Appl. Phys. 115 (2014) 034104 (034104-1~034104-5).
15. D.M. Ramo, P.V. Sushko, and A.L. Shluger, Phys. Rev. B 85 (2012) 024120 (024120-1~024120-10).
16. K. Hasekawa, P. Ajmet, N. Okazaki, T. Hasekawa, K. Fujimoto, M. Watanabe, T. Chikyow, and H. Koinuma, Appl. Surf. Sci. 223 (2004) 229-232.
17. J.H. Choi, Y. Mao, and J.P. Chang, Mater. Sci. Eng. R 72 (2011) 97-136.
18. D.C. Hays, B.P. Gila, F. Ren and S.J. Pearton, J. Vac. Sci. Technol. B 33 (2015) 061209 (061209-1~061209-6).
19. P.H. Carey, IV, F. Ren, D.C. Hays, B.P. Gila, S. Jang, A. Kuramata, and S.J. Pearton, Jap. J. Appl. Phys. 56 (2017) 071101 (071101-1~071101-5).
20. M.A. Quevedo-Lopez, M. El-Bouanani, R.M. Wallace, and B.E. Gnade, J. Vac. Sci. Eng. A 20 (2002) 1891-1897.
21. D.R. Lide, “CRC Handbook of Chemistry and Physics” (CRC Press, 2005).